Processing of printed silver patterns on an ETFE substrate

Processing of printed silver patterns on an ETFE substrate

Riikka Mikkonen*, Sanna Lahokallio†, Laura Frisk†, Matti Mäntysalo*
*Laboratory of Electronics and Communications Engineering,
Tampere University of Technology, Tampere, Finland
Email: riikka.mikkonen@tut.fi
†Trelic Ltd, Tampere, Finland
Email: sanna.lahokallio@trelic.fi

Abstract—Printed electronics makes it possible to fabricate devices on thin and flexible substrates at a low cost and with simple processing. However, substrate characteristics can make patterning challenging. Here, we report our approach for processing printed silver patterns on an extremely hydrophobic ethylene-tetrafluoroethylene (ETFE) foil substrate. The effects of selected surface modification methods on substrate characteristics and final print quality were studied, and the thermal characteristics of ETFE were determined. Conductive silver patterns were fabricated using both screen printing and inkjet printing techniques. Additionally, intense pulse light method was compared to thermal annealing as an alternative annealing method. The surface modification of ETFE was observed to affect ink wetting and print quality. It was concluded that the impact of the chosen annealing method on the final characteristics of the printed structures was significant.

Keywords—Printed electronics; ETFE; IPL; DSC; TMA

I. INTRODUCTION

In the last twenty years, ethylene-tetrafluoroethylene (ETFE) has gained popularity in architecture for its light transmission abilities, which are comparable to those of glass [1,2]. Other advantages include chemical resistance and an anti-stick surface with a self-cleaning ability [1,2]. Additionally, ETFE is lightweight, and thus, it is both safer and easier to handle as a building material than glass. Examples of well-known ETFE-based buildings include the Eden project in Cornwall, Domaquarée in Berlin, Kapuzinergraben in Aachen, Kingsdale School in London, and the Avenues mall in Kuwait [1,2]. High tear resistance and flexibility make this material attractive for other industries as well. Another important application area for ETFE is wire and cable insulation [3].

A contributing factor to its anti-stick and self-cleaning properties is the extremely low surface energy, being approximately 15–20 mN/m [4,5]. On the other hand, ETFE's hydrophobic surface is extremely difficult to coat, and in several approaches the material's hydrophobic characteristics have been utilized to produce anti-stick molds without friction [6-8]. However, Miesbauer et al. [9] coated ETFE foils with a special primer and zinc tin oxide (ZTO) in order to investigate ETFE foil-based encapsulation characteristics in organic photovoltaic (OPV) applications. They concluded that ETFE and other fluoropolymers can be used in OPV encapsulation when dimensional instability at high temperatures is compensated for, for example, by polymer lamination. In [10], aluminum oxide, peel adhesion was measured on both native ETFE and on modified ETFE. Peel adhesion was promoted with surface treatments, but the long-term effect was not studied.

In addition to OPVs, ETFE is an attractive substrate material for printed electronics (PE) applications. By printing electronics onto ETFE, large area electronics could be integrated into buildings. This approach would enable the direct integration of, for example, an intelligent lighting system onto roofs or walls.

Here, the effects of surface modifications on the ETFE surface characteristics were investigated, and their impact on ink wetting on ETFE was characterized. Additionally, DSC (differential scanning calorimetry) and TMA (thermomechanical gravity analysis) measurements were used to determine ETFE's thermal characteristics. Furthermore, an annealing method's effect on final trace performance was studied by using both a conventional thermal curing and an intense pulse light (IPL) annealing method.

II. MATERIALS AND METHODS

A. Materials

Commercial Novoflon ET 6235 EZ foils, produced by NOVOFOL Kunststoffprodukte GmbH & Co., were used in these experiments. Native ETFE was compared to corona pre-treated ETFE foil. According to manufacturer information, the melting point of the ETFE foils is 265°C, and the maximum operating temperature is 150°C, where 0–5% shrinkage may occur after 10 minutes exposure.

To minimize heating damage to the foil, low-temperature printing inks were selected for these experiments. Conductive silver traces were both inkjet printed and screen printed. Essential ink parameters, according to manufacturer information, are listed in Table 1.

B. Surface pre-treatments

To modify the surface characteristics of a hydrophobic ETFE foil, we used several surface pre-treatments: oxygen plasma, UV/ozone, and corona pre-treatments. Oxygen plasma treatment is a widely used method by which a surface can be activated by an increment of functional groups, consequently increasing surface energy and improving adhesion [11,12].

Even challenging surfaces can be modified with plasma, even though modification of fluorinated polymers has proven to be a challenge in previous approaches [13,14]. Here, we used an Oxford Plasma Technology RIE System 100 for vacuum plasma treatment with oxygen.

TABLE 1. INK PARAMETERS.

Ink	*Viscosity [mPa*s]*	*Ag [wt%]*	*Particle size*	*Curing conditions*	*Resistivity [Ωcm]*
Harima NPS-JL (inkjet)	90	55	7 nm	120°C/60min	6×10^{-6}
Novacentrix HPS-021LV (screen)	>1000	75	2–4 µm	150°C/30min	5.18×10^{-6}

Additionally, we used a 30-minute UV/ozone treatment with a Novascan PSD UVOP system. UV/ozone cleaning is used to increase the surface energy of hydrophobic materials, such as polydimethylsiloxane (PDMS), and thus, to promote wetting and adhesion [15-18]. We also corona pre-treated native ETFE with a roll-to-roll Vetaphone corona system in order to compare it with the commercial corona pre-treatment. A summary of the treatment parameters is given in Table 2.

TABLE 2. SURFACE PRE-TREATMENT PARAMETERS.

Oxygen plasma				
	Time [min.]	*Exposure power [W]*	*Chamber pressure [mTorr]*	*Gas amount [sccm]*
a	2	75	56	30
b	5	75	56	30
UV/ozone				
Time (min.)				
30				
Corona				
Exposure power (kW)			***Speed (m/min)***	
3.4			60 m/min	

C. Printing and curing

A Harima NPS-JL nanoparticle silver ink was inkjet printed with a piezoelectric Dimatix DMP-2831 tabletop inkjet printer. Plate and cartridge temperatures were kept at 40°C. A Novacentrix HPS-021LV flake silver ink was screen printed with a semi-manual TIC SCF300 device. We used an NBC Meshtec screen with 81 µm mesh openings and 45 µm thread diameters. Both devices were operated in clean room conditions.

After printing, samples were annealed, using either thermal annealing in an oven or the IPL annealing method. We used a Xenon Sinteron 2010-L system in the IPL annealing experiments. Samples were dried in a vacuum oven at 50–60°C for 15–30 minutes before the IPL annealing.

Business Finland Grant No. 2742/31/2016, Academy of Finland Grants No. 288945 and No. 294119.

D. Characterization

1) Surface energy and wetting

For the surface energy characterization, ETFE foil surface energy was measured as received. Additionally, the surface energies of the pre-treated samples were measured right after treatments. Further measurements were conducted after storage for 2 h, 4 h, 20 h, and 24 h to see if the obtained effect would fade over time. We measured the surface energies with a Dyne Pen set from Dyne Testing. This set contains 16 pens, covering surface energies ranging from 30 mN/m to 60 mN/m (in units of two, that is, 30, 32, 34…mN/m).

For the ink-wetting characterization, we inkjet printed the NPS-JL ink onto the native ETFE, the corona-treated ETFE, the UV/ozone-treated ETFE, and oxygen plasma-treated ETFE. A 25 µm drop spacing was used to compare ink wetting on each substrate. These samples were dried in the vacuum oven at 100°C for 60 minutes to prevent foil deformation and to enhance solvent evaporation in the vacuum environment. Additionally, wetting of the aqueous HPS-021LV ink was investigated on both the native and the corona pre-treated ETFE. Pattern quality and wetting were investigated with an optical microscope (an Olympus BX60m).

2) Thermal characteristics

As mentioned above, the Novoflon ET 6235 EZ foils' melting temperature is stated to be 265°C, and the maximum operating temperature is 150°C (where 0–5% shrinkage may occur). To confirm the thermal characteristics of these ETFE foils, we used DSC and TMA measurements. By DSC, the melting point was determined, and by the TMA measurement, we determined the glass-transition temperature T_g and also investigated the shrinkage tendency. Additionally, TMA was .used to determine the coefficient of thermal expansion (CTE) of ETFE below and above the glass-transition point.

The DSC measurements were conducted with a Q1000 system from TA Instruments. Two samples were heated (with a ramp rate of 20°C/min) from -40°C to 300°C. A TA Instruments Q400EM system was used for the TMA measurements. The ETFE foils were cut to strips and clamped to a film probe. The length of the samples was measured while heating the samples from -10°C to 200°C, with a ramp rate of 3°C/min. Three samples were measured, and for each of them, two consecutive heating runs were conducted.

3) Cured patterns

We evaluated the electrical performance of the cured traces by resistance measurements, where a Fluke 115 True-RMS multimeter and a 4-point probe (4PP) measurement system were used. A Keithley 2425 multimeter was used to measure the resistance with the 4PP system, and the sheet resistance R_s was calculated:

$$R_s = R(w/l), \quad (1)$$

where R is the measured resistance, l is the trace length, and w is the trace width. Additionally, we evaluated ink adhesion on ETFE by an ASTM-D3359 crosscut test.

III. Results and Discussion

A. Surface energy and ink wetting

In Table 3, the measured surface energies for the native and the pre-treated ETFE surfaces are presented. We observed that the oxygen plasma treatment had the most significant effect on the surface energy right after treatment. However, the surface energy started to recover. Finally, the surface energy of all the plasma-treated samples stabilized to approximately 40 mN/m with the 2-minute treatment and to 50 mN/m with the 5-minute treatment.

With the UV/ozone treatment, the surface energy increased to 54–56 mN/m, but started to recover after the treatment. After 24-hour storage in room temperature, the surface energy decreased significantly. Additionally, we noticed that the recovery was rather uneven: we measured surface energy values ranging from 34 mN/m to 42 mN/m on one sample after 24 h storage.

On the other hand, change in the surface energy with our corona pre-treatment was rather modest; the surface energy after the treatment was approximately 30–34 mN/m. However, the surface energy was maintained at this level, even after samples were stored at 22–24°C temperature and 20-30% relative humidity for 24 hours. Samples were wrapped in clean room paper to avoid excessive contamination. We obtained similar surface energies from the commercial corona pre-treated foil, and modification was observed to be permanent, even though the treatment appears to be slightly uneven: there are areas on the ETFE's surface on which the surface energy is below 30 mN/m.

TABLE 3. MEASURED SURFACE ENERGIES OVER TIME.

Time after exposure	***0 h***	***2 h***	***4 h***	***24 h***
Substrate	***Surface energy [mN/m]***			
Native ETFE	<<30	-	-	-
Plasma a	≥60	50–52	46	38–40
Plasma b	≥60	54–56	54–56	48–50
UV/ozone	54-56	50–52	44–48	34–42
Corona	30-34	30–34	30–34	30–34

After the surface treatments, we used both inks to pattern both the native and the corona pre-treated ETFE. In Fig. 1, the observed effects on the NPS-JL ink wetting are presented. The effect of the extremely low surface energy of the native ETFE is clear in Fig. 1a, where the contact angle between the ink and the substrate is very high and, thus, the ink cannot wet the ETFE surface in order to form continuous lines. In comparison, wetting is improved significantly with both the corona and the UZ/ozone treatments (Figs. 1b and 1c) and printed traces are continuous. In addition, drop spacing could still be kept at 25 µm, thus allowing the printing of narrow traces. On the other hand, modification by plasma treatment was clearly not suitable for the high-definition inkjet-printed lines: non-bulging patterns were only obtained when the drop spacing was increased to at least 60 µm (from the original 25 µm). Furthermore, well-defined traces with smooth edges were only obtained when drop spacing was increased further, to 80 µm and 100 µm.

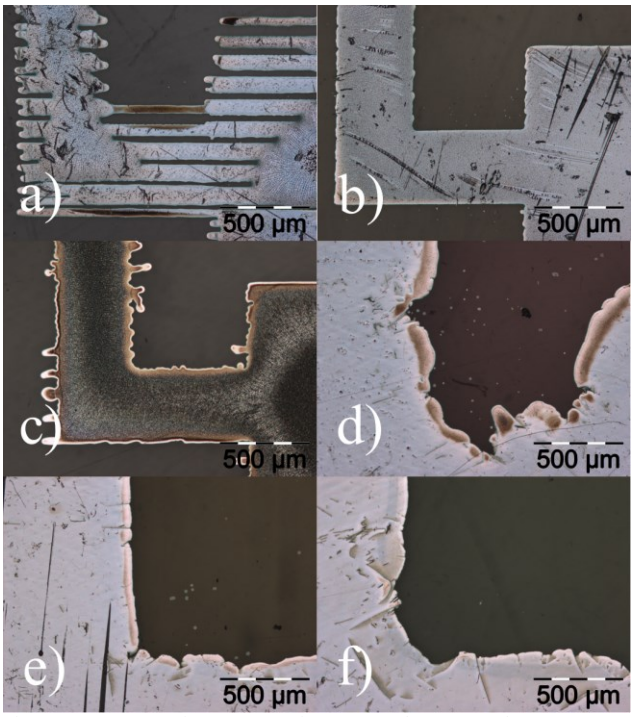

Fig. 1. NPS-JL wetting on a) native ETFE, ds: 25 µm, b) corona pre-treated ETFE, ds: 25 µm, c) UV/ozone treated ETFE, ds: 25 µm, d) plasma treated ETFE, ds: 60 µm, e) plasma treated ETFE, ds: 80 µm, and f) plasma treated ETFE, ds: 100 µm.

With screen printed patterns the effect was not as significant. However, we observed that the aqueous HPS-021LV ink could not wet the ETFE surface properly: several pinholes were observed in the cured silver structure, as demonstrated in Fig. 2. However, the corona pre-modification was effective enough for the printing of continuous patterns with smooth edges.

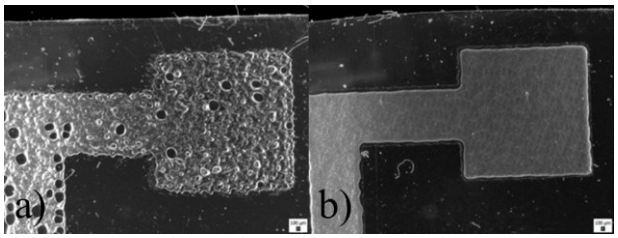

Fig. 2. HPS-021LV ink wetting on a) native ETFE, b) corona pre-treated ETFE. Scale bar: 100 µm.

B. ETFE thermal properties

The DSC measurement curves for the two ETFE samples are presented in Fig. 3. Similar behavior during heating runs was observed between samples. No significant changes in heat flow were observed until approximately 200°C, where the slope slightly changes, indicating the starting point of a phase transformation. A clear valley in the DSC signal is detected in the temperature area from approximately 235°C to 270°C, where the material melts. The determined ETFE melting points are shown in Table 4. Based on these results, it was concluded that the melting point is close to the stated 265°C.

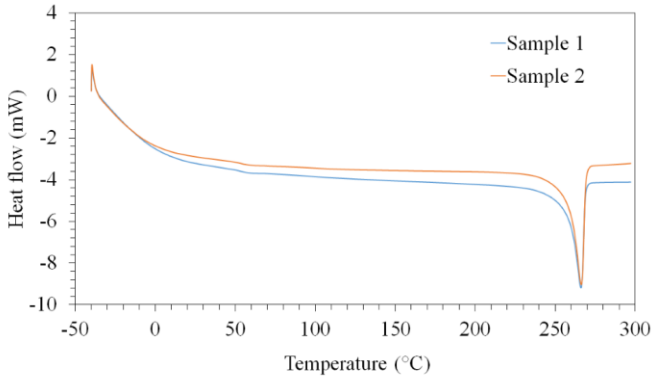

Fig. 3. ETFE heat flow as a function of temperature.

TABLE 4. DETERMINED MELTING POINTS.

Sample	Melting point [°C]
1	266.21
2	266.07

The TMA measurement curves for both heating runs and the three measured samples are shown in Fig. 4. As shown, the curves for the first and the second heating runs differ from each other. The first heating run's curves show that ETFE starts to shrink around 50–60°C. In this area, the sample softens, indicating that the T_g range of the material is reached.

The first heating curves include the thermal history, such as the internal stresses originating from the processing of the film. Because of this, the slopes of the first run differ from those of the second run from approximately 50°C to 150°C, after which no additional shrinkage occurs. In the second run, the thermal history has been removed and no shrinkage is seen. Additionally, no clear T_g can be seen. This is most likely due to the high crystallinity of the ETFE material and is typical behavior for fluoropolymers during the second heating run. Thus, T_g appears along the wide area between 50°C and 150°C and its exact range cannot be determined. However, because of the T_g range on the second heating run, the slope was not fully linear.

The CTE was determined from the second heating run, below and above T_g, by approximating the location of T_g from the change in the slope. The CTE values below and above T_g, and their averages are listed in Table 5. Shrinkage of the film was analyzed by comparing the lengths of the ETFE samples between the first and the second heating run. The shrinkage was determined at room temperature, and measured values are listed in Table 6. There was some variation in the shrinkage between the samples.

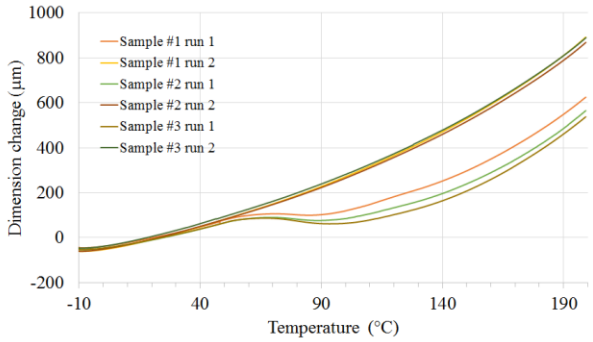

Fig. 4. TMA curves for all the measured samples.

TABLE 5. DETERMINED CTE VALUES, BELOW AND ABOVE T_G.

Sample	CTE below Tg [ppm/°C]	CTE above Tg [ppm/°C]
#1	137	361
#2	136	343
#3	138	346
Average	137	350

TABLE 6. SHINKAGE AFTER HEATING AT ROOM TEMPERATURE.

Temperature	Shrinkage in percentage [%]		
	Sample #1	*Sample #2*	*Sample #3*
22°C	1.20	1.39	1.58

C. Annealing

1) Thermal annealing

In these experiments, printed traces were cured at 100°C for 60 minutes, at 130°C for 30 minutes, and at 150°C for 30 minutes. We observed that curing at higher temperatures caused ETFE deformation: foils showed waviness when cured at 130°C or at a higher temperature, being completely curled when cured at 150°C. In addition to foil deformation, foils softened significantly. As a result, crosscut tests were impossible to conduct on these foils. We also observed that the

cured ink could be removed from the native ETFE foil with just a gentle scratching with the cutting tool, indicating severe adhesion issues. On the corona-treated ETFE, the ink layer remained intact after cutting, but the ink was removed completely by the adhesive tape.

Foil deformation and adhesion issues are most likely caused by the thermal characteristics of the ETFE foils: the T_g area appears between 50°C and 150°C, and thermal history causes shrinkage of the foils during heating. Additionally, the determined CTE is very high and increases with temperature. Since substrates with 20–30 ppm/°C in room temperature are typically used in printed electronics [19], it seems that there is a severe mismatch of the thermal characteristics of the used inks and the ETFE foils, causing ink delamination and affecting foil deformation.

Even though we did not observe foil deformation after post-processing at 100°C, the annealed traces were not conductive at all, or were only poorly conductive, when resistance was measured. Poor conductivity was observed, especially with the NPS-JL ink, where nanoparticles are used. Heating is critical for proper nanoparticle sintering, and therefore, the annealing temperature was clearly too low for this ink. In contrast, the aqueous matrix of the HPS-021LV ink can be evaporated effectively at 100°C and since flake sintering is not required, resistances were rather low. However, these resistances are not sufficient for high frequency (HF) applications or for illumination systems, such as light emitting diode (LED) matrix interconnections, where high conductivity is essential.

2) IPL annealing

To test the IPL annealing effects on pattern performance, several curing conditions were used for both the inkjet and the screen printed traces. In Table 7, the parameter combinations used for Novacentrix HPS-021LV screen printing ink are listed. The printed patterns were pre-dried in the vacuum oven at 60°C for 15 minutes before the IPL annealing. A one-second period of time was used, since it was the shortest possible period time with the used voltages and pulse lengths.

We observed that the chosen IPL parameters had a significant impact on the final print quality and trace topology. In Fig. 5, examples of too high and optimized parameters in terms of trace topology are presented. The trace in Fig. 5a has been cured using a 2.25 kV pulse voltage with a four-pulse burst, where the pulse length was 1 ms and the overall duration was 4 s, whereas the sample in Fig. 5b was cured with a 2.5 kV pulse voltage and with one 2 ms pulse. With the lower pulse voltage and the shorter pulse time, the trace surface and line edges remained relatively smooth and well defined, whereas a higher voltage, together with a long pulse time, caused bubbling on the conductor surface, probably due to poorly controlled, rapid solvent evaporation. Additionally, the line edges are rough and ink withdrawal towards higher ink density was observed. Furthermore, with the highest possible exposure powers, the annealed ink was even torn off from the ETFE surface by the impact of the light pulse. To optimize solvent evaporation and trace annealing with the IPL process further, we used a pre-drying step, where all the samples were placed to a vacuum oven for 15 minutes at 60°C. This additional step improved the final trace topology and yield via improved process control.

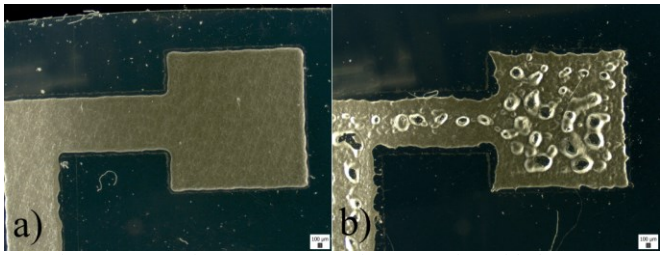

Fig. 5. Trace surface, HPS-021LV after IPL curing with the IPL parameters of a) set 7 and b) set 8.

The HPS-021LV results in Fig. 6 demonstrate the importance of the pulse length and the voltage on the final sheet resistance. The reference results are sheet resistance values, which we have previously measured when this ink was printed on a polyphenylene ether (PPE) substrate and annealed at 150°C for 30 minutes. We observed that similar or even lower sheet resistance values could be obtained with IPL, but only when using a 2 ms pulse. With a shorter pulse time, there is less deviation in the measurement results, but values below 20 mΩ/sq could not be obtained. Still, these higher values are sufficient for most printed electronics structures, even though they cannot be utilized efficiently in sensitive HF applications.

Furthermore, we observed that when using the highest voltages together with the highest possible pulse lengths, the ETFE surface showed signs of color alteration, indicating thermal damage. These alterations were parallel to the lamp direction, and therefore, it can be assumed that the resulting pulse power is too high for the ETFE foils. The thermal resistance of the foils might be improved with a suitable barrier layer on the ETFE's surface.

TABLE 7. HPS-021LV IPL PARAMETERS.

Set	*Voltage [kV]*	*Pulse count [N]*	*Pulse length [ms]*
1	2.00	1	1
2	2.00	2	1
3	2.00	4	1
4	2.20	2	2
5	2.25	1	1
6	2.25	2	1
7	2.25	4	1
8	2.50	1	1
9	2.50	2	1
10	2.50	4	1
11	2.50	2	2
12	3.00	1	2

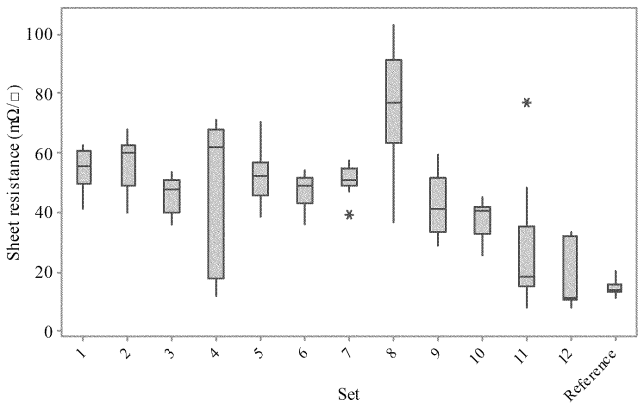

Fig. 6. HPS-021LV sheet resistances with different IPL parameter sets.

The NPS-JL annealing parameters were chosen by preliminary tests, where several curing parameters were used to compare effects. In Table 8, these preliminary IPL parameters and the measured resistances are presented. We fabricated ten samples for each set. All patterns were pre-dried in the vacuum oven at 60°C before IPL annealing: one-layer prints were appealed for 15 minutes and two-layer prints for 30 minutes. Again, a 1 s period of time was used. The parameter selection for the further experiments was based on both the obtained resistance and the sample survival rate. Here, the samples have been classified as having "survived" if the traces were still continuous and conductive after annealing. We observed that with the higher intensities in particular, parts of the traces tended to blow off, whereas with the lower intensities, the samples were less conductive. No great difference in resistance was observed between the one-layer prints and the two-layer prints. A thickness of one layer is around 700 nm, and thus, the ink volume does not increase significantly with two-layer printing. Therefore, the effect on resistance is not that significant either.

TABLE 8. IPL PARAMETERS AND THE RESULTS OF THE PRELIMINARY TESTS WITH NPS-JL INK.

Set	*Layers*	*Parameters*	*Total curing energy [J]*	*Measured resistance [Ω]*	*Surviving samples*
1	1	2 kV, 1ms x 4	1376	20–100	6
2	2	2 kV, 1ms x 4	1376	6–30	8
3	1	2 kV, 1ms + 2ms	1032	7–50	10
4	2	2 kV, 1ms + 2ms	1032	9–42	5
5	2	2 kV, 1.5ms x 4	2064	4–60	7
6	1	2.25 kV, 1ms + 2ms	1369	6–21	5
7	2	2.25 kV, 1ms + 2ms	1369	4–18	5
8	1	2.25 kV, 2ms + 2ms	1825	5–7	5
9	2	2.25 kV, 2ms + 2ms	1825	5–11	7
10	1	2.5 kV, 1ms x 4	2350	7–13	8
11	2	2.5 kV, 1ms x 4	2350	9–15	6

Based on the preliminary results, we chose the parameters of the one-layer sets 5 and 9 since the sample-survival rate was excellent and low resistances were measured, even though a lot of variation was observed with set 9. We fabricated 30 new samples for each set to characterize the sheet resistance. The obtained sheet resistances are presented in Fig. 7. Here, sheet resistance—measured with the NPS-JL ink on a PPE substrate using similar pattern and printing parameters with ink annealed at 150°C for 60 minutes—is used as a reference. With the IPL annealing method, some of the measured values meet this reference value and are even lower. However, we observed some variation in the measured values after the IPL annealing, especially with the set 9 parameters. Additionally, the mean sheet resistance is a little higher than with the set 5 parameters. This is not surprising since the annealing energy is over two times lower, which causes issues with the process control.

We also fabricated samples for adhesion rating by using the ASTM-D3359 crosscut test. This time, samples could endure the cutting step prior to tape application well, without any ink removal. No change in the foil hardness was observed during cutting either. Interestingly, we observed almost no adhesion failures when the adhesive tape was peeled off, but the ink cohesion failed in almost every sample. When we measured the resistances of the ink layer remaining on the foil, and the ink layer removed by the tape, we observed that the topmost, removed part was less conductive than the bottommost part that remained on the ETFE surface. This result indicates that the ETFE was heated rapidly in the process. At the same time, the resistance of the topmost ink layer was observed to be highly dependent on the used IPL parameters: with optimized annealing conditions, resistance was only slightly higher than that of the bottom layer, whereas with the less effective pulse parameters, the difference was greater.

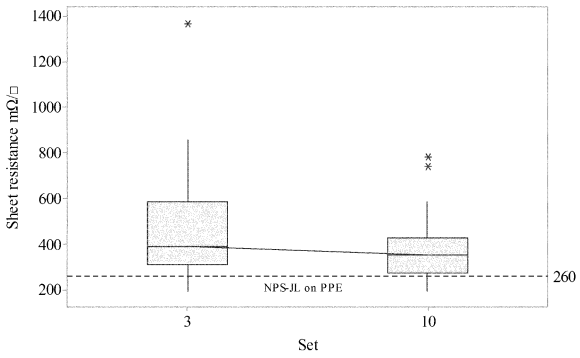

Fig. 7. NPS-JL sheet resistances after IPL curing. The measured sheet resistance of the PPE substrate is used as a reference.

Our results are in line with the earlier approaches [20-22], where it has been stated that the IPL sintering method can be effectively used on heat-sensitive substrates as an alternative annealing method. Obviously, trace performance is highly dependent on both the ink and the substrate characteristics, and process optimization is required for each material combination. On the other hand, the adhesion of IPL annealed structures has not been studied comprehensively. Considering

the delamination issues detected by both us and other authors, reaching a sufficient adhesion level and mechanical reliability by rapid IPL annealing may be rather challenging. Promoting adhesion is even more challenging on hydrophobic substrates, such as the ETFE foils studied here, and therefore, future research should focus on interface adhesion without damaging the substrate material.

IV. Conclusions

Here, the surface characteristics and the modification possibilities of commercial ETFE foils were determined. Additionally, thermal characteristics were determined by DSC and TGA measurements, and foil behavior during heat annealing of silver traces was investigated. Ink wetting and print quality were determined for native and pre-treated ETFE foils. Additionally, IPL annealing was used as an alternative method for the post-processing of printed silver patterns.

It was observed that ETFE is dimensionally unstable at temperatures above 100°C due to the low glass-transition temperature and the very high coefficient of thermal expansion above the glass-transition area. Additionally, challenges in ink wetting were observed on the native ETFE, but wetting promotion was obtained with the used surface pre-treatments. The IPL method was successfully used to anneal conductive traces without ETFE deformation.

Further investigation is required in order to promote ink adhesion on ETFE. First, the ink adhesion on ETFE should be studied in order to solve the issues related to the hydrophobic substrate surface. Second, the adhesion after IPL annealing should be investigated in order to ensure the sufficient adhesion and the mechanical reliability of the cured traces.

Acknowledgment

This work was funded by Business Finland Grant No. 2742/31/2016. M. M. is supported by the Academy of Finland Grant Nos. 288945 and 294119. We would like to thank Heikki Liejumäki from Tampere University of Technology, Faculty of Biomedical Sciences and Engineering for conducting the DSC experiments.

References

[1] J. Hu, W. Chen, B. Zhao, D. Yang, “Buildings with ETFE foils: a review on material properties, architectural performance and structural behavior,” Consctr. Build. Mater., vol. 131, pp. 411–422, 2017.

[2] C. Maywald, F. Riesser, “Sustainability – the art of modern architecture,” Procedia Eng., vol. 155, pp. 238–248, 2016.

[3] S. Lee, J-S. Park, R. Lee, “The wettability of fuoloropolymer surfaces: influence of surface dipoles,” Langmuir, vol. 24, pp. 4817–4826, Januray 2008.

[4] H. Teng, “Overview of the development of of the fluoropolymer industry”, Appl. Sci., vol. 2, pp. 496–512, May 2012.

[5] S H. Ahn, L. J. Guo, “Large-area roll-to-roll and roll-to-plate nanoimprint lithography: a step toward high-throughput application of continuous nanoimprinting”, ACS Nano, vol. 3, pp. 2304–2310, 2009.

[6] G. Ding, K. Wang, X. Li, Q. Chen, Z. Hu, J. Liu, “The Fabrication of nanoimprinted P3HT nanograting by patterned ETFE mold at room temperature and its application for solar cell”, Nanoscale Res. Lett., vol. 11, May 2016.

[7] D. N. Weiss, S. T. Meyers, D. A. Keszler, “All-inorganic thermal nanoimprint process”, J. Vac. Sci. & Technol., B: Nanotechnol. Microelectron.: Mater., Process., Meas., and Phenom., vol. 28, June 2010.

[8] B. Kwon, J. H. Kim, “Importance of molds for nanoimprint litography: hard, soft and hybrid molds”, J. Nanosci., vol. 2016, ID 6571297, 2016.

[9] O. Miesbauer, M. Pfrogner, C. Steiner, J. Fahlteich, K. Noller, “Multilayer barrier structures on ETFE susbtrate films,” AIMCAL Web Coating & Handling Conference Europe, Dresen, Germany, 30.5.–2.6. 2016.

[10] J. Fahlteich et al., “Roll-to-roll thin film coating on fluoropolymer webs-status, challenges and applications,” Surf. Coat. Technol., vol. 314, pp. 160–168, March 2017.

[11] P. K. Chu, J. Y. Chen, L. P. Wang, N. Huang, “Plasma-surface modification of biomaterials,” Mater. Sci. Eng., R, vol. 36, pp. 143–206, March 2002.

[12] S. Guruvenket, G. M. Tao, M. Komath, A. M. Raichur, “Plasma surface modification of polystyrene and polyethylene,” Appl. Surf. Sci., vol. 236, pp. 278–284, September 2004.

[13] A. Vesel, M. Mozetic, A. Zalar, “XPS characterization of PTFE after treatment with RF oxygen and nitrogen plasma,” Surf. Interface Anal., vol. 40, pp. 661–663, Januray 2008.

[14] N. Iganaki, “Surface modification of ethylene-co-tetrafluoroethylene copolymer (ETFE) by plasma,” Nucl. Instrum. Methods Phys. Res., Sect. B, vol. 208, pp. 277–280, August 2003.

[15] A. Delplanque, E. Henry, J. Lautru, H. Leh, M. Buckle, C. Nogues, “UV/ozone surface treatment increases hydrophilicity and enhances functionality of SU-8 photoresist polymer,” Appl. Surf. Sci., vol. 314, pp. 280–285, September 2014.

[16] A. Oláh, H. Hillborg, G. J. Vansco, “Hydrophobic recovery of UV/ozone treated poly(dimethylsiloxane): adhesion studies by contact mechanics and mechanism of surface modification,” Appl. Surf. Sci., col 239, pp. 410–423, Januray 2005.

[17] K. Efimenko, W. E. Wallace, J. Genzer, “Surface modification of Sylgard-184 poly(dimethyl siloxane) networks by ultraviolet and ultraviolet/ozone treatment,” J. Colloid and Interface Sci., col. 254, pp. 306–315, October 2002.

[18] Y. Berdichevsky, J. Kahndurina, A. Guttman, Y-H. Lo, “UV/ozone modification of poly(dimethylsiloxane) microfluidic channels,” Sens. Actuators, B, vol. 97, pp. 402–408, February 2004.

[19] S. Khan, L. Lorenzelli, R. S. Dahiya, ”Technologies for printing sensors and electronics over large flexible substrates: a review,” IEEE Sens. J., vol. 15, pp. 3164–3185, June 2015.

[20] S. Wünscher, R. Abbel, J. Perelaer, U. S. Schubert, “Progress of alternative sintering approaches of inkjet-printed metal inks and their application for manufacturing of flexible electronics,” J. Mater. Chem. C, 00, pp. 1–25, 2014.

[21] W-H. Chung, H-J. Hwang, S-H. Lee, H-S. Kim, “In situ monitoring of a flash light sintering process using silver nano-ink for producing flexible electronics,” Nanotechnology, vol. 24, ID 035202, December 2012.

[22] J. Niittynen, R. Abbel, M. Mäntysalo, J. Perelaer, U. S. Schubet, D. Lupo, ” Alternative sintering methods compared to conventional thermal sintering for inkjet printed silver nanoparticle ink,” Thin Solid Films, vol. 556, pp. 452–459, April 2014.